ZIBELINE INTERNATIONAL™ PUBLISHING

ISSN: 2521-0920 (Print)
ISSN: 2521-0602 (Online)
CODEN: MJGAAN

Malaysian Journal of Geosciences (MJG)

DOI: http://doi.org/10.26480/mjg.02.2025.146.153

RESEARCH ARTICLE

3-D GEO-CELLULAR MODEL OF A LOW NET-TO-GROSS FLUVIAL OUTCROP: IMPLICATIONS OF FACIES-SCALE SEDIMENTARY HETEROGENEITY ON STATIC PROPERTIES IN RESERVOIR ANALOGUES

Bayonle A. Omoniyi*, Olakunle Kayode, and Afolabi Dolapo

Department of Earth Sciences, Adekunle Ajasin University, Akungba-Akoko, Nigeria
**** Corresponding author: bayonle.omoniyi@aaua.edu.ng***

ARTICLE DETAILS

Article History:

Received 19 August 2025
Revised 27 September 2025
Accepted 15 October 2025
Available online 13 November 2025

ABSTRACT

This study focusses on geological modelling of a fluvial outcrop analogue, illustrating the impact of stratigraphic architecture on sand-body distribution, internal geometry, and stacking on sedimentary heterogeneity and static properties. Outcrop measurements and sedimentological logs generated from a 4.8 km²-section provide data for modelling two lithostratigraphic zones from the three zones recognised. The model consists of a Cartesian grid with 576 cells and 544 cells in the horizontal directions. Each cell is 5 m x 5 m along horizontal directions and 4.3 m along depth. Facies object method was used for modelling lithology and Sequential Gaussian Simulation for modelling porosity and permeability data sourced from a subsurface analogue. The results reveal that a major channel element in Zone 1 has complex ribbon geometry marked by upward thinning and fining sequences. In this zone, intraformational mudrock rip-up clasts form channel lags with potential as flow baffles in pebbly sandstone intervals while thick floodplain mudrock limits lateral continuity of interbedded sandstone, posing huge risks to lateral sweep. Crevasse splays in Zone 2 improve lateral continuity of interbedded sandstone. However, mud-prone heterolithic deposits may pose a significant risk to vertical sweep in poorly connected splay intervals. Therefore, drilling horizontal laterals from existing wells into such intervals and/or adopting a gas-based depletion strategy may improve areal sweep in previously bypassed low-connectivity zones. In hydrocarbon fields where overbank sheets are sandwiched between thick floodplain fines, exemplified by Zone 3, in-place volume may be uneconomic to warrant development.

KEYWORDS

Sand-body architecture, internal geometry, geological modelling, flow barriers, fluvial reservoir.

GRAPHIC ABSTRACT

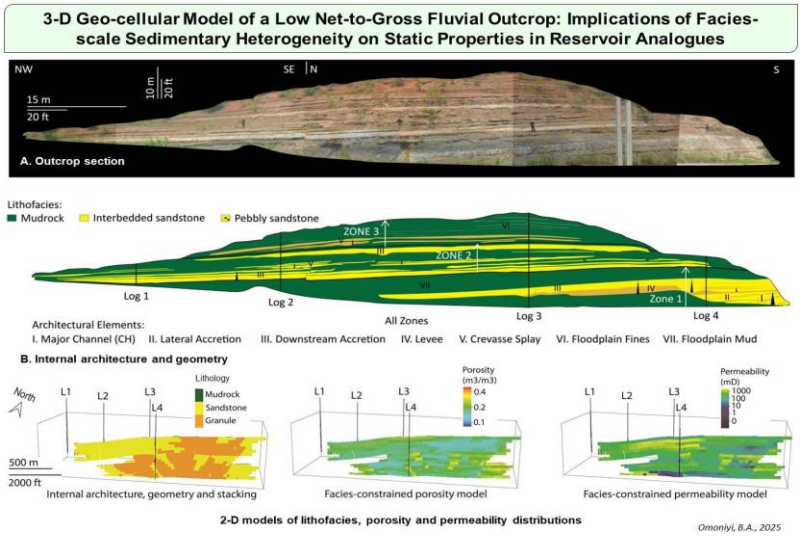

Quick Response Code	Access this article online	
	Website: www.myjgeosc.com	**DOI:** 10.26480/mjg.02.2025.146.153

Cite the Article: Bayonle A. Omoniyi, Olakunle Kayode, and Afolabi Dolapo (2025). 3-D Geo-Cellular Model Of A Low Net-To-Gross Fluvial Outcrop: Implications Of Facies- Scale Sedimentary Heterogeneity On Static Properties In Reservoir Analogues. Malaysian Journal of Geosciences, 9(2): 146-153.

1. Introduction

1.1 Background

Hydrocarbon-bearing fluvial sediments form important reservoirs in many sedimentary basins (Atkinson et al., 2006; Dixon et al., 2010). These sediments are mainly deposited by meandering or braided rivers within the channel fairway and/or in the overbank. Braided channels are typically formed in wide braid-plain systems and are characterised by high sediment discharge (Miall, 2014). Meandering channels, by contrast, form in channel systems that are more mature with relatively low sediment flux. The axis and margin of meandering channels consist of channel-fill sequences, whereas in the overbank, sequences with mounded morphology develop as levees or sheet morphology as crevasse splays (Bridge, 2003; Hudson, 2017; Omoniyi, 2021). Discharge variability in river systems prompts changes in depositional architecture (Manna et al., 2021) and thus influences sedimentary organisation, stratigraphic framework, internal geometry and dimension of sand bodies (Burns et al., 2010; Soltan and Mountney, 2016; Willis and Sech, 2018). These geological attributes exert a strong control on net-to-gross, continuity, porosity and permeability of sandstone and sand-rich heterolithic bodies in fluvial reservoirs, and therefore sway their reservoir potential and recovery factor (Pranter et al., 2007). Discontinuous shale in fluvial reservoirs disposes them to relatively low recovery factor because of the complex internal geometry of respective sand bodies causing significant quantities of hydrocarbon to be bypassed in low-connectivity reservoir intervals in many mature fields (e.g. Wytch Farm oil field, United Kingdom; Hogg et al., 1999, etc.).

Fluvial reservoirs are among the most complex reservoirs and their hydrocarbon potential varies considerably in response to variability in stratigraphic framework and internal geometry of sand bodies (North and Prosser, 1993). In particular, low net-to-gross fluvial reservoirs are marked by high rate of change of lithology and petrophysical properties, reservoir architecture (a product of depositional and diagenetic processes that developed the reservoir), internal fabric and dimensions of sand bodies that not only make subsurface geological description and prediction extremely difficult, but ultimately control the paths of fluid flow during hydrocarbon production. Understanding these geological attributes and distribution of sporadic permeability barriers allow proper description of sedimentary heterogeneity that pave the way for liberation of trapped hydrocarbons (Puig et al., 2019). According to (Tyler and Finley 1991), geological heterogeneity traps up to 40% of moveable oil reserves in fluvial reservoirs, and this proportion is arguably higher in low net-to-gross fluvial reservoirs. Beyond these problems, crevasse-splay deposits, although are difficult to find and define, constitute a significant component of the overbank successions, up to 90% and may contain significant reserves in many fields that are producing from low net-to-gross fluvial reservoirs (Burns et al., 2017).

Over the last four decades, geological-integrated reservoir modelling has seen tremendous growth with capabilities to locate reservoir areas that have potential as stratigraphic compartments where hydrocarbon fluids are trapped. But, these subsurface reservoir models are limited by the available geological information (Howell et al., 2014). Outcrop analogues provide a means to understand variability and distribution of geological properties and hence improve our understanding of depositional architecture of sedimentary systems (Pranter et al., 2014; Siddiqui et al., 2018; Usman et al., 2021). This information is routinely used to supplement subsurface geological data (Sahoo et al., 2016; Zhou et al., 2017; Stow et al., 2020). And, to derive geometrical parameters that serve as building blocks for three-dimensional (3-D) property modelling (Fabuel-Perez et al., 2010). The resultant models are the groundwork for simulating fluid flow and predicting shale discontinuity and other stratigraphic heterogeneity in subsurface analogue reservoirs (Willis and White, 2000; Larue and Friedmann, 2005).

Although rock record analogues are associated with the problems of scales when compared with subsurface reservoir analogues due to relatively small size of exposures (Alexander, 1993). They provide the basis for understanding reservoir rock distribution, stratigraphic architecture, sandbody heterogeneity, distribution of internal impermeable barriers, etc. and aid qualitative and/or semi-quantitative prediction of attributes of reservoir rocks (Pranter et al., 2014, Rittersbacher et al., 2014; Villamizar et al., 2015; Newell and Shariatipour, 2016). Therefore, this study utilizes outcrop measurements and geological attributes to describe architectural elements in a low net-to-gross fluvial succession and used the information to build 3-D models that capture sand-body architecture and internal geometry. The primary objective of the study is to describe lithostratigraphic framework of the fluvial body, model internal geometry and distribution of sand bodies, and assess implications of sedimentary heterogeneity on static properties of these bodies, and by extension, appraise associated risks to hydrocarbon recovery.

1.2 Geological Setting

The fluvial body utilised in this study outcrops between Latitudes N 07011'03.1'' and N 07011'06.7'', and Longitudes E 006028'02.7'' and E 006028'04.1'' along Okpekpe-Igodo township road in Edo North, southern Nigeria. It consists of Campanian-Maastrichtian successions in western flank of Anambra Basin (Figure 1). The intracratonic basin is a post-Santonian depocentre that extends from the Lower Benue Trough covering an estimated area of 40,000 km^2 and accumulating sediments, up to 5,000 m thick, derived from a wide spectrum of paleoenvironmental settings (Nwajide and Reijers, 1996). The trough is a rift structure that originated about the same time as the opening of the South Atlantic Ocean when the Gondwana Supercontinent broke in late Jurassic times (Offodile, 1989). Omoniyi and Imagbe (2025), following previous workers, present a synthesized description of stratigraphy of the Anambra Basin. The 4.8 km^2 section is composed of sand bodies that are enclosed by mudrock (Figure 2). Barring a 3.1 m (10 ft)-long normal fault observed in the middle section, the fluvial body is largely unaffected by tectonic activity. Apart from this rationale, the siliciclastic body is a classic example of low net-to-gross fluvial system associated with well-developed overbank sheet bodies.

2. Material And Method

Four sedimentological logs were produced from outcrop observations and measurements. The logs were considered adequate to collect geological attributes of sand bodies and to quantify dimensions of sand-body architecture, model lithology distribution, define depositional elements and internal geometry. They serve as basis for correlation and provide information over vertical extent of the outcrop on lithology, sandstone-mudstone ratio, net-to-gross, grain size and sorting, small-scale sedimentary structures, and small-scale vertical sequences of bed thickness. These attributes enable classification of lithology into three broad sediment facies (i.e. lithofacies) and construction of lithostratigraphic framework.

The "facies" represents a body of rock that possesses a combination of characteristics, which serve to differentiate the rock unit from related rock units above, below and laterally adjacent, and usually reflect the origin of a rock unit (Walker, 1992). The differentiating factor for lithofacies in this study is lithology distribution, which forms the basis for contextualizing sedimentary architecture of the fluvial body. The exposed part of the fluvial body was carefully and safely traced laterally and vertically to establish irregularity in bed thickness and gather data on internal geometry and morphology of sand bodies. The information influenced selection of the most geologically consistent correlation scheme for further study and enabled recognition of three zones. Two of these zones were modelled using object model technique in Schlumberger Petrel™. The technique requires lithofacies data, morphology and geometry data (shape, width, direction, and thickness) to build in space whole objects with their specific geometries (Labourdette et al., 2008; Colombera et al., 2019). Object densities were adapted to local proportions to achieve net-to-gross and volume proportion targets. The rationale for applying object-based modelling to simulate depositional facies spatial distribution is to mimic the geological reality observed and documented during fieldwork. Because of the consistency in facies geometry, only one lithofacies realisation was considered. This realisation is the groundwork for modelling lithofacies and depofacies (i.e. depositional facies). The actual thickness, width and position of the depofacies (main channel, crevasse splay, and floodplain) vary along the channel. A 3-D block-centred Cartesian grid was designed for modelling these properties. The grid comprises 576 cells and 544 cells in the horizontal directions. Each grid cell has dimensions of 5 m x 5 m along horizontal directions and 4.3 m along depth. Grid cells are top horizon conformable to reflect deposition of sediment in a channel while capturing macroscopic-scale (10-100 m) sedimentary heterogeneity without the need for upscaling in subsequent modelling phase.

Porosity and permeability data sourced from a subsurface. This simulation estimates of reservoir properties beyond known points and realisation of spatial distribution of the data (Ringrose and Bentley, 2015). One lithofacies-constrained porosity and permeability distribution realisation was run on a set of parameters (Table 1) to investigate hydrocarbon pore volume in the two zones. Insights from these models were used to conceptualise oil production scenario with a view to assessing risk of bypassing oil in poorly connected and/or isolated oil-bearing sand bodies.

3. Results And Discussion

3.1 Results

3.1.1 Lithofacies classification

Sedimentary facies distribution is one of the dominant factors that control

fluid flow through a sand body. Fluid migration through a sand body is reduced by discontinuous, relatively impermeable barriers, such as shale lenses, which increase tortuosity of fluids through the sand body (Tyler and Finley, 1991; Puig et al., 2019). Based on dominant lithology, grain size, sedimentary structures, and nature of bedding, recognise fifteen lithofacies in the fluvial body. For modelling purpose, the lithofacies are grouped into three: (1) pebbly sandstones, (2) interbedded sandstones, and (3) mudrocks (Figure 3).

Pebbly sandstones consist of sandstone and clasts of various composition, most commonly quartz, and sizes, ranging in dimensions from 4.5 cm to 15.2 cm long and 0.5 cm to 7.5 cm wide. The clasts are arranged without any preferred orientation in a matrix of fine-to-coarse grained sandstone. The lithofacies make about 31% of the outcrop and display internal grading. Sorting is generally poor but improves in the upper part. Internal organisation is dominated by scour and fill, wavy subparallel bedding, trough cross lamination, ripple lamination, and ripple cross lamination. Amalgamation of pebbly sandstone beds increases bed thickness up to 3.0 m. Net-to-gross across various intervals is reduced to an average of 70% by dispersed shards of claystone that form basal lags and randomly distributed mud-prone load balls with dimensions of 30-40 cm long and approximately 10 cm wide.

Interbedded sandstones account for 19.8% of the rock exposure and comprise variable proportion of non-net lithology. They are distinguished by variable bed thicknesses that range from 0.2 m to 1.5 m and extend laterally up to 45.0 m across the width of the exposure before thinning out into a blanket of mudrock. The heterolithic lithofacies comprise medium-to-coarse- grained sandstone that is poor-to-moderately sorted and is interbedded with shale or claystone. They have lower net-to-gross (50-65%) and lower visible porosity than pebbly sandstones (<20%). Associated with these lithofacies are tabular bedding, wavy subparallel bedding, discontinuous wavy-to-non-parallel lamination, ripple lamination, ripple cross lamination, flaser lamination, and less commonly, convoluted lamination that emanated from excess sand deposition with minor mud.

Mudrocks consist of claystone, shale, and mudstone with infrequent siltstone lenses that imprint on it a wispy lamination in places. They have a relative abundance of 49.2% in the fluvial body and typically occur as wispy laminated claystone, structureless claystone, wavy laminated mudstone, lenticular laminated shale, and mudrock clasts. They serve as background lithofacies into which massive lenticular-bedded very coarse-grained sandstone is incised. Elsewhere, they occur as laterally extensive mudrock containing sporadic carbonaceous material and interbeds of planar subparallel-bedded clayey sandstone. Individual beds are separated by discontinuous silt streaks and lenses and may be up to 1.3 m thick and 100 m wide. Mudrock clasts of various sizes occur intermittently and as rip-up clasts at lower sections of scour-filled sandstone.

3.1.2 Architectural elements, porosity, and permeability

The lithostratigraphic framework based on selected correlation scheme reflects a high degree of variability in sand-body geometry and dimension, continuity, and stacking pattern (Figure 4). On this basis, seven architectural elements are recognised in the fluvial body: major channel, lateral-accretion deposit, downstream-accretion deposit, levee, crevasse splay, floodplain fines, and floodplain mud (Figure 5). These elements are grouped for geological modelling purpose into three, namely: (a) Channel Elements (2) Overbank Elements (3) Floodplain Elements, and they represent the principal depositional facies in the fluvial body. Two of the three zones recognised were selected for geological modelling.

The lithofacies models for Zones 1 and 2 captured by the lithostratigraphic framework reflect distinct lithofacies distribution trends, allowing strong deterministic control that perfectly captures the geological concept and architectural elements. Pebbly sandstones dominate channel-fill sequences in the two zones and represent mud-to-sand-prone heterolithic facies in the main channel, whereas interbedded sandstones, which extend from channel margin to overbank, dominate crevasse splay sequences as sandstone-to-sand-prone. Mudrocks represent background lithofacies, occurring as floodplain fines and mud. Porosity and permeability models reflect a strong control of lithofacies on distribution of these properties. Pebbly sandstones in channel-fill sequences are the most porous and mudrocks are the least porous. Sand bodies that are constrained within channel margin and proximal overbank are typified by higher porosity and permeability than poorly sorted clay-clasts-rich pebbly sandstones in the channel axis.

3.2 Discussion

3.2.1 Depositional architecture and sand-body connectivity

Connectivity pathways created by reservoir quality sand bodies are critical to effective fluid recovery (Howell et al., 2014). Fluvial sand bodies are internally complex and may present a huge challenge during reservoir development. In fact, a seemingly uniform sheet of high-permeability sand may actually turn out to be composed of many irregularly distributed clay rip- up clasts that drape the basal parts to create discontinuity surfaces and thus compartmentalise otherwise continuous reservoirs. The complexity of fluvial depositional systems controls their stratigraphic architecture and sand-body geometry and dimensions (Miall, 2014). The fluvial body is marked by low net-to-gross, complex sand-body architecture and internal geometry that reflect attributes of sediments deposited in a meandering river channel (van Toorenenburg et al., 2016).

Zone 1 is composed of a major channel and within-channel elements that occur as lateral-accretion and downstream-accretion deposits. The channel element exhibits a complex ribbon geometry that scoured into underlying floodplain mudrock to develop upward-thinning and upward-fining sedimentary sequences. The upward-fining trend in grain size is indicative of a progressive loss of river energy, through time, within the river channel, and caused finer and finer-grained sediments to be deposited as the flow velocity decreased gradually (Slatt, 2013; Miall, 2014). The vivid grey colour exhibited by the mudrock (shaly and occasionally carbonaceous) in this zone indicates the prevalence of waterlogged reducing conditions (Jones and Glover, 2005). The sand body and the overlying mudrock make up a 10 m-thick major channel sequence, which is marked mostly by fairly continuous pebbly sandstones that pass upward to coarse sandstones, forming characteristic vertically stacked channel fills. This stacking pattern is enhanced by bed amalgamation and it is prominent in the channel axis. Channel sandstones are composed of tabular cross-beds that are 0.5-0.8 m long and lenticular- shaped scours that are 5-6 m wide and 0.3-3.0 m high. The scour and fills are composed of trough cross-bedded sandstones that are mainly medium-to-coarse-grained and pebbly in places. The major channel elements are distinguished by broad and flat erosive bases that are overlain by mud-prone load casts, and are made up of stepped margins. Based on the fine-grained sandstones to lenticular-bedded granular-to-pebbly sandstones that dominate sediment infilling in the stepped channel margins, the sequence is interpreted to have been deposited during falling stages of meandering river flow (Friend and Sinha, 1993; Collinson and Mountney, 2019). Field observations showed the tendency of sandstone bodies to amalgamate increases with increasing lithofacies proportion. In this regard, appreciable lateral continuity of sand bodies in upper part of the channel element creates lateral stacking in contrast to lower part where isolated stacking develops as a result of progressive confinement of pebbly sandstones downsystem. Although pebbly sandstones thin away from the channel axis to the overbank, increasing net-to-gross associated with lateral continuity of channel sandstones into the overbank area where they accumulate as crevasse splays enhances connectivity between laterally-stacked interbedded sandstones and vertically-stacked pebbly sandstones (van Toorenenburg et al., 2016).

Zone 2, by contrast, comprises lateral accretion deposits displayed as sheet sand bodies. These sheet bodies have flat bounding surfaces and lack erosional features, suggesting deposition in the floodplain by poorly channelised or unstable channelised flow. Average width- to-height ratio of the sandbodies is 15. Aside from these lateral accretion deposits, the zone consists of lens-shaped sandstone that fills broad and shallow scours to form 2.5-3.0 m-thick and 6.0-7.5 m wide sedimentary fills. These scours have simple ribbon geometry and are interpreted as crevasse channels while the associated sheet sand bodies are interpreted as crevasse splays. Together, they represent overbank elements and their deposition is linked to poorly channelised or unstable channelised flow that breached the channel margin, carrying and depositing extensive bedload sediments. In this zone, there are discontinuous tabular-bedded sandstone beds that are up to 0.5 m thick and are frequently sandwiched between two extensive sheet sand bodies within a blanket of floodplain fines. These discontinuous bodies form distal overbank sheets, extending from proximal crevasse splay to distal crevasse splay. The orientation of the accretion surface and that of the cross-bedding in the downstream-accretion element ranges, implying accumulation of sheet sand bodies by accretion in a direction that was parallel to local flow. Floodplain fines that separate these sandstones imprint on an isolated stacking pattern, to poor vertical connectivity.

Zone 3 succeeds Zone 2 and tops the fluvial body. This zone comprises distal overbank sandstone sheets that are less than 0.5 m thick and are blanketed by thick sequences of floodplain fines (more mud than silt). The presence of fine lamination and very small ripples in the sandstone sheets suggests deposition by suspension during a waning flood regime (Galloway and Hobday, 1996; Stow, 2005). The zone has low net-to-gross (<20%) and correspondingly very poor visible porosity (<15%), and therefore has poor reservoir quality.

3.2.2 Implications for hydrocarbon recovery

Fluvial sand bodies favour accumulation of hydrocarbon fluids, but how

much of the hydrocarbon volume is connected remains uncertain because of uncertainty in their internal architecture, which makes it difficult to model and predict fluid flow in subsurface analogue reservoirs (Issautier et al., 2014). Although it is important to locate sand-rich channel elements in low net-to-gross fluvial bodies, establishing degree of connectivity between these channel elements determines hydrocarbon recovery (Larue and Friedmann, 2005; Ringrose and Bentley, 2015). Beyond establishing the degree of connectivity, numerous clay-draped discontinuity surfaces that develop irregularly across basal parts of fluvial reservoirs not only complicate flow models but also make fluid flow predictions inaccurate even in otherwise continuous sheet sandstone reservoirs. Outcrop-based integrated geocellular modelling can improve understanding of the variability in channel bodies' geometry and dimensions for better characterisation of subsurface analogue reservoirs (Enge et al., 2007; Howell et al., 2014, Pranter et al., 2014).

Fluvial sandbodies with typical complex ribbon geometry and internal architecture dominated by sand and mud within well-defined meander belts, as exemplified by Zone 1, are commonly associated with well-developed point bars, crevasse splays, and mud-rich channel plugs within extensive floodplain mudrock (Miall, 2014). In these belts, there is a difficult arrangement of sand pods, lenses, and channels that results in a complex labyrinth of interconnected sand bodies, even when they extend laterally over several hundreds of metres (Sahoo et al., 2016; Colombera et al., 2017). Zone 70 of the Sherwood Sandstone reservoir in Wytch Farm oil field, United Kingdom, is a classic example of subsurface analogue that depicts this stratigraphic architecture and sand-body geometry. The zone comprises a 20 m-thick floodplain mudrocks and sand-rich channel-fills (Hogg et al., 1999). Despite the compound ribbon geometry and characteristic vertical stacking of sandstones in this zone, channel lags with intraformational mudrock rip-up clasts overlying basal erosional surface pose a huge risk to vertical communication as flow baffles (Newell and Shariatipour, 2016). Aside from the risk of flow baffling, such sequences may lack overbank sheets in crevasse splays and thus be capped by thick floodplain mudrock that restricts lateral continuity of good quality interbedded sandstones from channel margin to proximal overbank (Figure 6). In the presence of discontinuous sandstone sheets, effectiveness of horizontal sweep of hydrocarbon by injected water, in this instance, is largely uncertain. However, vertical connectivity between two point bars may improve where floodplain mudrocks do not totally separate them areally and/or there are proximal sand-rich crevasse splays observed in Zone 2 (Donselaar and Overeem, 2008; van Toorenenburg et al., 2016). The presence of crevasse splays in this zone improves lateral continuity of good-quality sand bodies, but mud-prone heterolithic deposits between two splays may reduce vertical connectivity and therefore pose a significant risk to flow communication between two successive hydrocarbon-bearing splays (Figure 7). This is the case for Zone 30 in the Sherwood Sandstone reservoir where a 7 m-thick interval of splay sandstones is interbedded with mud-prone floodplain deposits (Hogg et al., 1999).

These results imply that potential of meandering fluvial reservoirs suffers where net-to- gross is low and reservoir-quality sand bodies are restricted (Figure 8). Subsurface analogues with internal architecture and geometry typified by Zone 3 usually have insufficient net sandstone to warrant consideration for development. Generally, the fining-upward trend that distinguishes vertical profile of point-bar sequences is associated with upward-decreasing permeability (Davies et al., 1993). Which is unfavourable to hydrocarbon recovery, and may cause injected water to preferentially flood high-permeability basal part of point bars while it bypasses uppermost low-permeability region (Jones et al., 1995; Pranter et al., 2007). As successfully carried out in the Wytch Farm oil field, water injection into existing aquifer provided pressure support and effectively swept oil from the relatively well-connected Lower Sherwood Sandstone. Where sandbody communication is poor, as is the case for Upper Sherwood Sandstone, horizontal laterals drilled from existing wells into un-drained reservoir intervals improved oil recovery at lower water cuts (Hogg et al., 1999). Beyond this depletion strategy, gas injection may prove more effective to reduce potential for bypassed oil in the upper low-connectivity areas, and therefore, ameliorate the problem of preferential flooding in producing fluvial reservoir analogues that have similar internal architecture.

4. Conclusions

Although ancient analogues are associated with problems of scales caused by relatively small size of exposures, they provide the basis for understanding reservoir rock distribution and aid qualitative and/or semi-quantitative prediction of reservoir behaviour. This study demonstrates the complexity of low net-to-gross fluvial body captured by facies variations, sand-body architecture, internal geometry and stacking, and rock property distribution in the two zones modelled.

Zone 1, composed of a major channel and within-channel elements, exhibits a complex ribbon geometry that scoured into underlying floodplain mudrock while forming upward- thinning and upward-fining vertically stacked successions of pebbly sandstones. Zone 2, by contrast, comprises sheet sand bodies with relatively flat bounding surfaces that lack erosional features. The sediment fill in this zone is attributed to deposition by poorly channelised or unstable channelised flow. However, the sediment fill is occasionally associated with sandstones that fill its broad and shallow scours forming lens-shaped sedimentary successions. Generally, the two zones are characterised by lateral thinning of bed thickness from channel axis to overbank. Unlike in Zone 1, sand bodies in Zone 2 are associated with increasing net-to-gross closely attributed to lateral continuity of channel sandstones into the overbank where they accumulate as crevasse splays. These splays enhance connectivity between laterally-stacked interbedded sandstones in Zone 2 and vertically-stacked pebbly sandstones in Zone 1. Zone 3, which tops the fluvial body, comprises distal overbank sheets sandwiched between thick intervals of floodplain fines and mud, and are considered non-reservoir because of low net-to- gross and very poor visible porosity.

Findings reveal that intraformational mudrock rip-up clasts overlying basal erosional surfaces may pose a huge risk to vertical communication in subsurface analogues that have similar internal architecture. Aside from this risk, absence of well-developed crevasse splays in subsurface analogues may deny them overbank sand sheets that would otherwise enhance interconnectivity of sand bodies for better hydrocarbon recovery. Furthermore, the thick floodplain mudrock that caps low net-to-gross fluvial body, as exemplified by this study, may restrict lateral continuity of good quality interbedded sandstones from channel margin to proximal overbank thereby increasing risk of poor horizontal sweep of hydrocarbon. When floodplain fines and mud (mud-prone heterolithic deposits) do not totally separate sand bodies areally and/or there are proximal sand-rich crevasse splays, vertical communication between two successive hydrocarbon-bearing layers may be significantly enhanced. While more data are necessary to improve understanding of the distinctive productive zones and minimize risk of flow baffles/barriers in low net-to-gross fluvial reservoirs, three-dimensional geometry, orientation, spatial distribution and total volume of net sand bodies must be determined to develop and effectively manage hydrocarbon production in the long run.

Acknowledgements

The authors express gratitude to the anonymous reviewers for their valuable comments on the original manuscript.

References

Atkinson, C., Renolds, M., Hutapea, O., 2006. Stratigraphic traps in the Tertiary rift basins of Indonesia: case studies and future potential, in: Allen, M.R., Goffey, G.P., Morgan, R.K., Walker, I.M. (Eds.), The Deliberate Search for the Stratigraphic Trap. Geological Society, London, Special Publication 254, pp. 105-126, https://doi.org/10.1144/GSL.SP.2006.254.01.06

Dixon, R.J., Moore, J.K.S., Bourne, M., Dunn, E., Haig, D.B., Hossack, J., Roberts, N., Parsons, T., Simmons, C.J., 2010. Integrated petroleum systems and play fairway analysis in a complex Palaeozoic basin: Ghadames–Illizi Basin, North Africa, in: Vining, B.A., Pickering, S.C. (Eds.), Petroleum Geology: From Mature Basins to New Frontiers – Proceedings of the 7th Petroleum Geology Conference. Geological Society, London, pp. 735-760, https://doi.org/10.1144/0070735

Miall, A.D., 2003. Fluvial depositional systems. Springer, Cham. https://doi.org/10.1007/978-3-319-00666-6

Bridge, J.S., 2003. Rivers and floodplains: forms, processes, and sedimentary record. Blackwell Science, Oxford.

Hudson, P.F., 2017. Fluvial depositional processes and landforms, in: Richardson, D., Castree, N., Goodchild, M.F., Kobayashi, A., Liu, W., Marston, R.A. (Eds.), The International Encyclopedia of Geography. John Wiley and Sons, 2017, pp. 1-9, https://doi.org/10.1002/9781118786352.wbieg0872

Omoniyi, B.A., 2021. Fluvial facies and their reservoir potential: a concise review. Science Research and Engineering Development 4(4), 1255-1266.

Manna, M.O., Scherer, C.M.S., Bállico, M.B., dos Reis, A.D., Moraes, L.V., Ferrari, L.A.B., Roisenberg, H.B., de Oliveira, V.G., 2021. Changes in fluvial architecture induced by discharge variability, Jaicós Formation (Silurian-Devonian), Parnáiba Basin, Brazil. Sedimentary Geology 420, 105924, https://doi.org/10.1016/j.sedgeo.2021.105924

Burns, E.R., Bentley, L.R., Hayashi, M., Grasby, S.E., Hamblin, A.P., Smith, D.G., Wozniak, P.R., 2010. Hydrogeological implications of paleo-fluvial architecture for the Paskapoo Formation, SW Alberta, Canada: a stochastic analysis. Hydrogeology 18, 1375-1390, https://doi.org/10.1007/s10040-010-0608-y

9Soltan, R., Mountney, N.P., 2016. Interpreting complex fluvial channel and barform architecture: Carboniferous Central Pennine Province, northern England. Sedimentology 63, 207-252.

Willis, B.J., Sech, R.P., 2018. Quantifying impacts of fluvial intra-channel-belt heterogeneity on reservoir behaviour, in: Ghinassi, M., Colombera, L., Mountney, N.P., Reesink, A.J.H. (Eds.), Fluvial Meanders and Their Sedimentary Products in the Rock Record. International Association of Sedimentologists Special Publication 48, pp. 543-572.

Pranter, M.J., Ellison, A.I., Cole, R.D., Patterson, P.E., 2007. Analysis and modeling of intermediate-scale reservoir heterogeneity based on a fluvial point-bar outcrop analog, Williams Fork Formation, Piceance Basin, Colorado. American Association of Petroleum Geologists Bulletin 91(7), 1025-1051, https://doi.org/10.1306/02010706102

Hogg, A.J.C, Evans, I.J., Harrison, P.F., Meling, T., Smith, G.S., Thompson, S.D., Watts, G.F.T., 1999. Reservoir management of the Wytch Farm Oil Field, Dorset, UK: providing options for growth into later field life, in: Fleet, A.J., Boldy, S.A.R. (Eds.), Petroleum Geology of Northwest Europe: Proceedings of the 5th Conference. Geological Society, London, pp. 1157-1172, https://doi.org/10.1144/0051157

North, C.P., Prosser, D.J., 1993. Characterization of fluvial and aeolian reservoirs: problems and approaches, in: North, C.P., Prosser, D.J. (Eds.), Characterization of Fluvial and Aeolian Reservoirs. Geological Society, London, Special Publication 73, pp. 1-6.

Puig, J.M., Cabello, P., Howell, J., Arbués, P., 2019. Three-dimensional characterisation of sedimentary heterogeneity and its impact on subsurface flow behaviour through the braided-to-meandering fluvial deposits of the Castissent Formation (late Ypresian, Tremp-Graus Basin, Spain). Marine and Petroleum Geology 103, 661-680, https://doi.org/10.1016/j.marpetgeo.2019.02.014

Tyler, N., Finley, R.J., 1991. Architectural controls on the recovery of hydrocarbons from sandstone reservoirs, in: Miall, A.D., Tyler, N. (Eds.), The Three Dimensional Facies Architecture of Terrigenous Clastic Sediments and its Implication for Hydrocarbon Discovery and Recovery. Society for Sedimentary Geology, Oklahoma, Concepts in Sedimentology and Paleontology 3, pp. 1-5.

Burns, C.E., Mountney, N.P., Hodgson, D.M., Colombera, L., 2017. Anatomy and dimensions of fluvial crevasse-splay deposits: Examples from the Cretaceous Castlegate Sandstone and Neslen Formation, Utah, U.S.A. Sedimentary Geology 351, 21-35, https://doi.org/10.1016/j.sedgeo.2017.02.003

Howell, J.A., Martinius, A.W., Good, T.R., 2014. The application of outcrop analogues in geological modelling: a review, present status and future outlook, in: Martinius, A.W., Howell, J.A., Good, T.R. (Eds.), Sediment-Body Geometry and Heterogeneity Analogue Studies for Modelling the Subsurface. Geological Society, London,, Special Publication 387, 1-25, https://doi.org/10.1144/SP387.12

Pranter, M.J., Hewlett, A.C., Cole, R.D., Wang, H., Gilman, J., 2014. Fluvial architecture and connectivity of the Williams Fork Formation: use of outcrop analogues for stratigraphic characterization and reservoir modeling, in: Martinius, A.W., Howell, J.A., Good, T.R. (Eds.), Sediment-Body Geometry and Heterogeneity: Analogue Studies for Modeling the Subsurface. Geological Society, London, Special Publication 387, pp. 57-83, https://doi.org/10.1144/SP387.1

Siddiqui, N.A., Ramkumar, M., Rahman, A.H.A., Mathew, M.J., Santosh, M., Sum, C.W., Menier, D., 2018. High resolution facies architecture and digital outcrop modeling of the Sandakan formation sandstone reservoir, Borneo: implications for reservoir characterization and flow simulation. Geoscience Frontiers, 1-15.

Usman, M., Siddiqui, N.A., Zhang, S., Mathew, M.J., Zhang, Y., Jamil, M., Liu, X., Ahmed, N., 2021. 3D geo-cellular static virtual outcrop model and its implications for reservoir petro-physical characteristics and heterogeneities. Petroleum Science 18, 1357-1369, https://doi.org/10.1016/j.petsci.2021.09.021

Sahoo, H., Gani, M.R., Hampson, G.J., Gani, N.D., Ranson, A., 2016. Facies- to sandy-scale heterogeneity in a tight-gas fluvial reservoir analog: Blackhawk Formation, Wasatch Plateau, Utah, USA. Marine and Petroleum Geology 78, 48-69.

Zhou, F., Shields, D., Titheridge, D., Tyson, S., Esterle, J., 2017. Understanding the geometry and distribution of fluvial channel sandstones and coal in the Walloon Coal Measures, Surat Basin, Australia. Marine and Petroleum Geology 86, 573-586, https://doi.org/10.1016/j.marpetgeo.2017.06.020

Stow, D., Nicholson, U., Kearsey, S., Tatum, D., Gardiner, A., Ghabra, A., Jaweesh, M., 2020. The Pliocene-Recent Euphrates river system: sediment facies and architecture as an analogue for subsurface reservoirs. Energy Geoscience 1, 174-193.

Fabuel-Perez, I., Hodgetts, D., Redfern, J., 2010. Integration of digital outcrop models (DOMs) and high resolution sedimentology - workflow and implications for geological modelling: Oukaimeden Sandstone Formation, High Atlas (Morocco). Petroleum Geoscience 16, 133-154, https://doi.org/10.1144/1354-079309-820

Willis, B.J., White, C.D., 2000. Quantitative outcrop data for flow simulation. Sedimentary Research 70(4), 788-802, https://doi.org/1073-130X/00/070-788

Larue, D.K., Friedmann, F., 2005. The controversy concerning stratigraphic architecture of channelized reservoirs and recovery by waterflooding. Petroleum Geoscience 11, 131-146, https://doi.org/10.1144/1354-079304-626

Alexander, J., 1993. A discussion on the use of analogues for reservoir Geology, in: Ashton, M. (Ed.), Advances in Reservoir Geology. Geological Society, London, Special Publication 69, pp. 175-194, https://doi.org/10.1144/gsl.sp.1993.069.01.08

Rittersbacher, A., Howell, J.A., Buckley, S.J., 2014. Analysis of fluvial architecture in the Blackhawk Formation, Wasatch Plateau, Utah, USA, using large 3D photorealistic models. Sedimentary Research 84, 72-87, https://doi.org/10.2110/jsr.2014.12

Villamizar, C.A., Hampson, G.J., Flood, Y.S., Fitch, P.J., 2015. Object-based modelling of avulsion-generated sandbody distributions and connectivity in a fluvial reservoir analogue of low to moderate net-to-gross ratio. Petroleum Geoscience 21, 249-270, https://doi.org/10.1144/petgeo2015-004

Newell, A.J., Shariatipour, S.M., 2016. Linking outcrop analogue with flow simulation to reduce uncertainty in sub-surface carbon capture and storage: an example from the Sherwood Sandstone Group of the Wessex Basin, UK, in: Bowman, M., Smyth, H.R., Good, T.R., Passey, S.R., Hirst, J.P.P., Jordan, C.J. (Eds.), The Value of Outcrop Studies in Reducing Subsurface Uncertainty and Risk in Hydrocarbon Exploration and Production. Geological Society, London, Special Publication 436, pp. 231-246, https://doi.org/10.1144/SP436.2

Murat, R.C., 1972. Stratigraphy and paleogeography of the Cretaceous and Lower Tertiary in southern Nigeria, in: Dessauvagie, T.F.J., Whiteman, A.J. (Eds.), African Geology. Ibadan, University of Ibadan Press, pp. 251-266.

Nwajide, C.S., Reijers, T.J.A., 1996. Sequence architecture in outcrops: examples from the Anambra Basin, Nigeria. Nigerian Association of Petroleum Explorationists Bulletin 11, 23-33.

Offodile, M.E., 1989. A review of the geology of the Cretaceous of the Benue Valley, in: Kogbe, C.A. (Ed.), Geology of Nigeria, second ed., Rock View, Jos, pp. 365-376.

Omoniyi, B.A., Imagbe, L.O., 2025. Anatomy and facies analysis of fluvial body, western flank of Anambra Basin, southern Nigeria: an outcrop study. Geography, Environment and Earth Science International 29(2), 43-65, https://doi.org/10.9734/jgeesi/2025/v29i2863

Walker, R.G., 1992. Facies, facies models and modern stratigraphic concepts, In: Walker, R.G., James, N.P. (Eds.), Facies Models: Response to Sea Level Change. Geological Association of Canada, Newfoundland, pp. 2-14.

Labourdette, R., Hegre, J., Imbert, P., Insalaco, E., 2008. Reservoir-scale 3D sedimentary modelling: approaches to integrate sedimentology into a reservoir characterization workflow, in: Robinson, A., Griffiths, P., Price, S., Hegre, J., Muggeridge, A. (Eds.), The Future of Geological Modeling in Hydrocarbon Development. Geological Society, London,

Special Publication 309, pp. 75-85, https://doi.org/10.1144/SP309.6

Colombera, L., Mountney, N.P., Medici, G., West, L.J., 2019. The geometry of fluvial channel bodies: empirical characterization and implica-tions for object-based models of the subsurface. American Associa-tion of Petroleum Geologists Bulletin 103(4), 905-929, https://doi.org/

10.1306/10031817417

Yaliz, A., 1991. The Crawford field, Block 9/28a, UK North Sea, in: Ab-botts, I.L. (Ed.), United Kingdom Oil and Gas Fields, 25 Years Com-memorative Volume. Geological Society, London, Memoir 14, pp. 287-293.

Ringrose, P., M. Bentley, 2015. Reservoir Model Design – A Practitioner's Guide. Springer, Berlin, https://doi.org/10.1007/978-94-007-5497-3

Jones, N.S., Glover, B.W., 2005. Fluvial sandbody architecture, cyclicity and sequence stratigraphic setting - implications for hydrocarbon reservoirs: the Westphalian C and D of Osnabrück-Ibbenbüren ar-ea, northwest Germany, in: Collinson, J.D., Evans, D.J., Holliday, D.W., Jones, N.S. (Eds.), Carboniferous Hydrocarbon Resources: the Southern North Sea and surrounding Onshore Areas. Geological Society, Yorkshire, 26 p.

Van Toorenenburg, K.A., Donselaar, M.E., Noordijk, N.A., Weltje, G.J., 2016. On the origin of crevasse-splay amalgamation in the Huesca fluvial fan (Ebro Basin, Spain): implication for connectivity in low net-to-gross fluvial deposits. Sedimentary Geology 343, 156-164.

Slatt, R.M., 2013. Stratigraphic reservoir characterization for petroleum geologists, geophysicists, and engineers: origin, recognition, initiation, and reservoir quality, second ed. Elsevier Developments in Petroleum Science, Amsterdam.

Friend, P.F., Sinha, R., 1993. Braiding and meandering parameters, in: Best, J.L., Bristow, C.S. (Eds.), Braided Rivers. Geological Society, London, Special Publication 75, pp. 105-111.

Collinson, J.D., Mountney, N.P., 2019. Sedimentary structures, fourth ed. Dunedin Academic Press, Edinburgh.

Galloway, W.E., Hobday, D.K., 1996. Terrigenous Clastic Depositional Systems: Applications to Fossil Fuel and Groundwater Resources, second ed. Springer-Verlag, Berlin, https://doi.org/10.1007/978-3-642-61018-9

Stow, D.A.V., 2005. Sedimentary rocks in the field: a colour guide. Man-son publishing, London.

Issautier, B., Viseur, S., Audigane, P., Le Nindre, Y.M., 2014. Impacts of fluvial reservoir heterogeneity on connectivity: implications in es-timating geological storage capacity for CO2. International Journal of Greenhouse Gas Control 20, 333-349, https://doi.org/10.1016/j.ijggc.2013.11.009

Colombera, L., Mountney, N.P., Russell, C.E., Shiers, M.N., McCaffrey, W.D., 2017. Geometry and compartmentalization of fluvial meander-belt reservoirs at the bar-form scale: quantitative insight from out-crop, modern and subsurface analogues. Marine and Petroleum Ge-ology 82, 35-55.

Donselaar, M.E., Overeem, I., 2008. Connectivity of fluvial point bar de-posits: an example from the Miocene Huesca fluvial fan, Ebro basin, Spain. American Association of Petroleum Geologists Bulletin 92(9), 1109–1129.

Davies, D.K., Williams, B.P.J., Vessell, R.K., 1993. Dimensions and quality of reservoirs originating in low and high sinuosity channel sys-tems, Lower Cretaceous Travis Peak Formation, East Texas, USA, in: North, C.P., Prosser, D.J. (Eds.), Characterization of Fluvial and Aeolian Reservoirs. Geological Society, London, Special Publication 73, pp. 95-121.

Jones, A., Doyle, J., Jacobsen, T., Kjønsvik, D., 1995. Which sub-seismic heterogeneities influence waterflood performance? A case study of a low net-to-gross fluvial reservoir, in: deHaan, H.J. (Ed.), New De-velopments in Improved Oil Recovery. Geological Society, London, Special Publication 84, pp. 5-18

APPENDICES

There is no appendix submitted with this paper.

FIGURE CAPTIONS

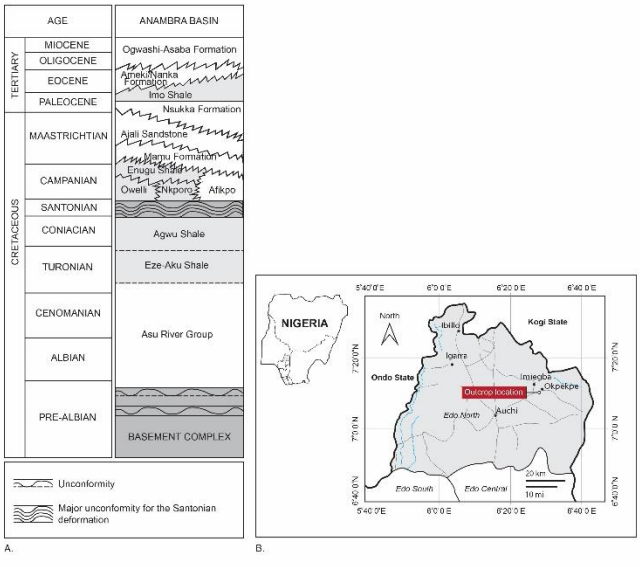

Figure 1. **(A)** Schematic stratigraphic succession of the Anambra Basin (after Murat, 1972 in Nwajide and Reijers, 1996). (B) Map of Edo North District where the fluvial body is located. Inset: Map of Nigeria showing Edo State. Geological map was reproduced from Geological and Mineral Resources Map of Edo State, Nigeria (Nigerian Geological Survey Agency, 2022).

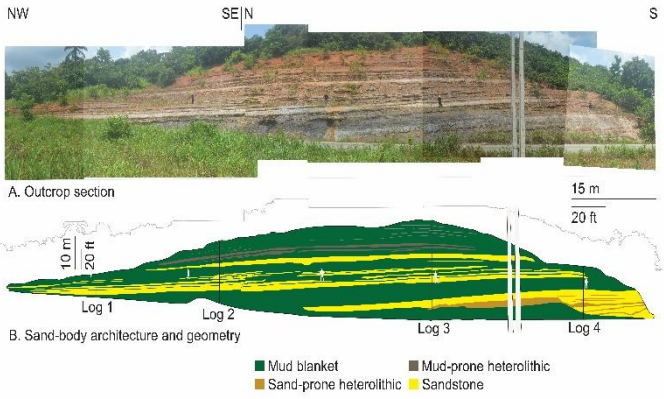

Figure 2. (A) Photograph of exposed part of the fluvial body. This part exceeds 4.8 km2 and consists of sand bodies that are blanketed by mudrock. (B) Sand-body architecture and geometry. Humans shown serve as vertical scale. The body is a classic ancient analogue for low net-to-gross fluvial deposits.

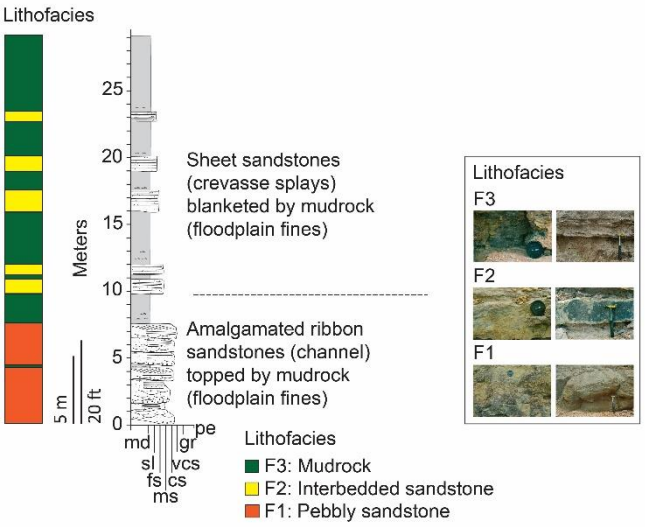

Figure 3. Schematic sedimentological model for the fluvial body. It is characterised by variability in sandstone internal geometry and dimensions. Photograph of principal lithofacies is shown to the right of the model. md = mud; sl = silt; fs = fine sand; ms = medium sand; cs = coarse sand; vcs = very coarse sand; gr = granule; pe = pebble.

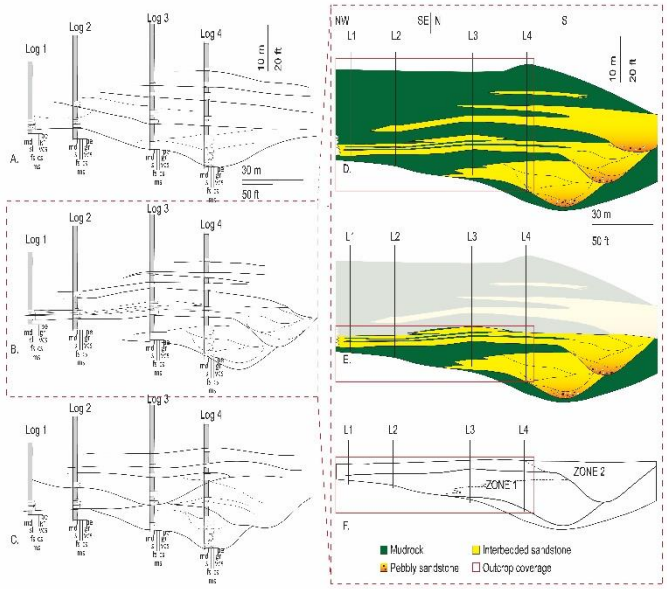

Figure 4. Correlation schemes (A-C) based on four sedimentological logs that capture outcrop observations and measurements. Correlation scheme B was selected based on its consistency with field observations to create a lithostratigraphic framework. The framework reveals three zones from which two zones were selected for geological modelling (D-F). These zones provide deterministic geometrical data for object modelling of lithofacies. The part of the framework and model structure (shown as thick red line in D-F) truly reflects the outcrop section shown in Figure 2, whereas the part outside the coverage in E and F was extrapolated based on interpretations of analogous ancient analogues (Miall, 1981, 2006, 2014). md = mud; sl = silt; fs = fine sand; ms = medium sand; cs = coarse sand; vcs = very coarse sand; gr = granule; pe = pebble.

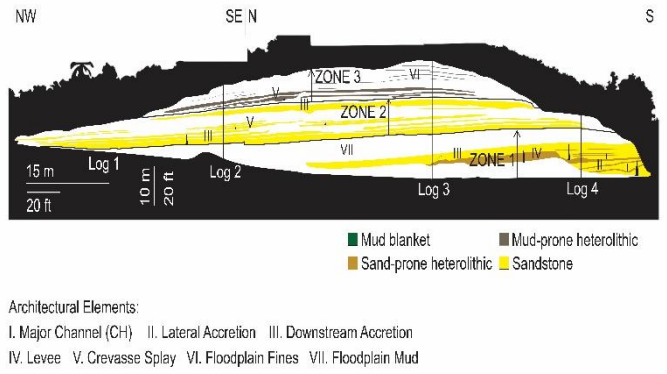

Figure 5. Schematic outcrop section illustrating architectural elements and lithostratigraphic divisions (Zones 1-3) recognised in the fluvial body. Zone 1 is characterised by complex ribbon geometry, whereas Zones 2 and 3 are distinguished by laterally continuous sheet sand bodies.

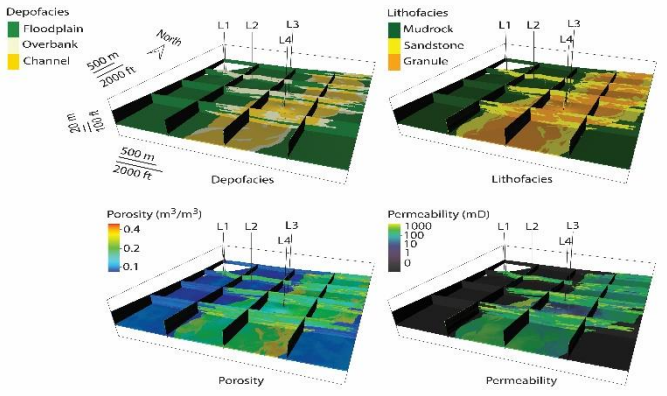

Figure 6. Fence diagrams produced from 3-D models of lithofacies depofacies, lithofacies, porosity, and permeability. Depofacies model shows variability in distribution of channel and overbank deposits enclosed within floodplain fines and mud. Granules and pebbly sandstones are primarily deposited within channel fairway while finer sandstones are deposited along channel margin and in the overbank. These sandstones extend beyond channel margin to form laterally continuous sand bodies in Zone 2. These sand bodies are attributed to sheetflood or poorly channelised flows. Porosity and permeability are highest in the channel off-axis and margin. All models honour available data.

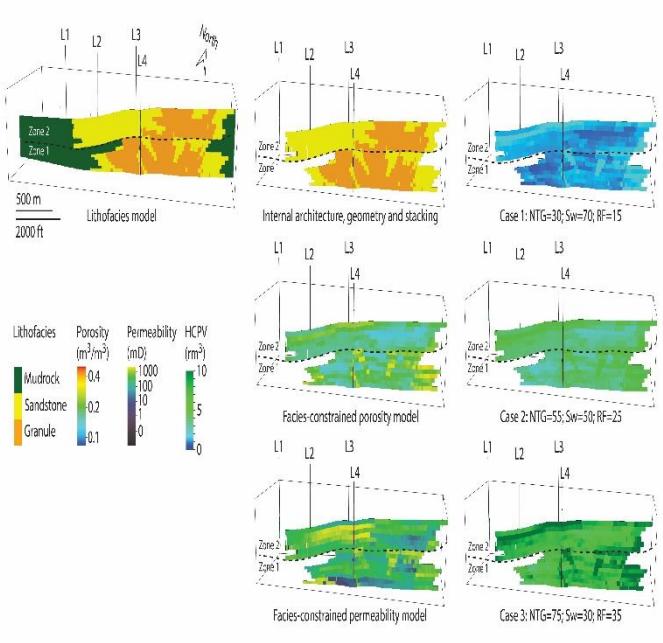

Figure 7. 2-D models illustrating variability in depofacies and lithofacies distributions and implications for porosity, permeability, and hydrocarbon pore volume (HCPV). The three cases considered reveal that sedimentary heterogeneity can affect distribution of hydrocarbon. This heterogeneity is largely influenced by distinctive sand-body architecture, internal geometry, and stacking that typify the two zones considered. Vertical connectivity of sand bodies is better in Zone 1 at high net-to-gross, whereas lateral connectivity is better in Zone 2 at a range of net-to-gross.

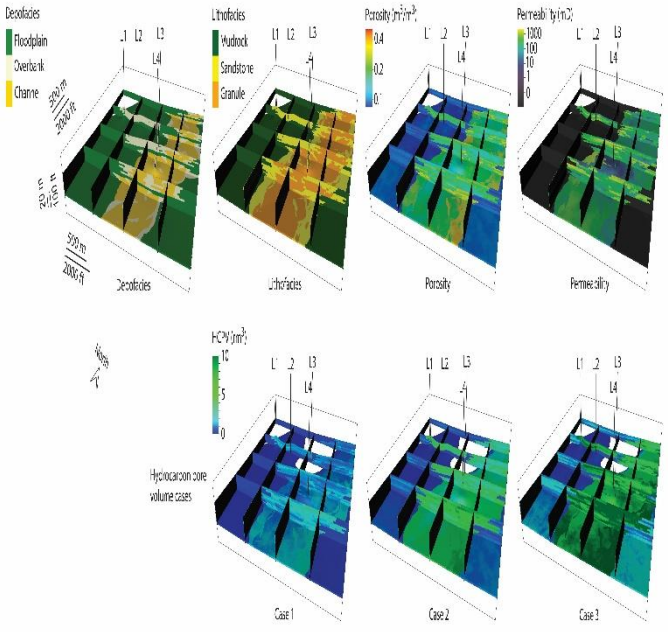

Figure 8. 3-D models illustrating variability in depofacies and lithofacies distributions and implications for porosity, permeability, and HCPV. Laterally continuous sand-rich sheet bodies in Zone 2 will support lateral communication between injection well and production well in reservoir analogues. However, this support is associated with a higher risk of high water production post breakthrough as injected water may rapidly advance to the production well after sweeping their oil. Beyond this pitfall, mud-prone heterolithic deposits that are sandwiched between two sheet sand bodies may reduce vertical communication between two potential pays.

Table 1: Parameters for object modelling.

Zones	Facies proportion		Porosity (m3/m3)	Permeability (mD)
	Raw	Upsccaled		
2	Channel = 20% Overbank = 80%	Channel = 3.1% Overbank = 85.4%	F3: Min. = 0.01 Max. = 0.05 Mean = 0.03 St. dev. = 0.03 F2: Min. = 0.15 Max. = 0.25 Mean = 0.20 St. dev. = 0.07 F1: Min. = 0.10 Max. = 0.20 Mean = 0.15 St. dev. = 0.07	F3: Min. = 0.001 Max. = 0.010 Mean = 0.006 St. dev. = 0.006 F2: Min. = 1.00 Max. = 2000.00 Mean = 1000.50 St. dev.= 1414.00 F1: Min. = 0.01 Max = 750.00 Mean = 375.05 St. dev. = 530.26
1	Channel = 25% Overbank = 75%	Channel = 41.3% Overbank = 14.8%	F3: Min. = 0.01 Max. = 0.05 Mean = 0.03 St. dev. = 0.03 F2: Min. = 0.18 Max. = 0.35 Mean = 0.27 St. dev. = 0.12 F1: Min. = 0.10 Max. = 0.25 Mean = 0.18 St. dev. = 0.11	F3: Min. = 0.001 Max. = 0.010 Mean = 0.006 St. dev. = 0.006 F2: Min. = 1.00 Max. = 2000.00 Mean = 1000.50 St. dev.= 1414.00 F1: Min. = 0.01 Max = 750.00 Mean = 375.05 St. dev. = 530.26